E3S Web of Conferences **410**, 02057 (2023)
FORM-2023
https://doi.org/10.1051/e3sconf/202341002057

Synthesis and characterization by experimental and theory research suitable on the CdS and CdO materials

I. B. Sapaev[1, 3*], *G. S.* Boltaev[1], *B.* Sapaev[2], *J. Sh.* Abdullayev[1], *S.* Sadullaev[1], *F. Kh.* Khasanov[1], and *N. O.* Akhmedjonov[4, 5]

[1]"Tashkent Institute of Irrigation and Agricultural Mechanization Engineers" National Research University, Tashkent, Uzbekistan
[2]Tashkent State Agrarian University, Tashkent, Uzbekistan
[3]New Uzbekistan University, Tashkent, Uzbekistan
[4]Nurafshan Branch of Tashkent University of Information Technologies Named After Muhammad Al-Khwarizmi, Uzbekistan
[5]Tashkent University of Information Technologies Named After Muhammad Al-Khwarizmi, Tashkent, Uzbekistan

Abstract. In this paper, we have compared and analyzed experimental and theoretical research on A^2B^6 types semiconductor materials CdS and CdO. The XRD spectra of the samples were examined using an atomic force microscope and X-ray diffraction microscopy. During film deposition, the temperature of the crucible with a source (CdS) varied in the range T_{sourse} ≈800 ÷ 850°C, and the substrate temperature was maintained within the range T_p ≈ 250 ÷ 270°C. In this case, to ensure the reproducibility of the structures, a shutter was used, with the help of which the CdS deposition time was set, which ensured that the film thickness was the same from experiment to experiment.

1 Introduction

Cadmium sulfide is a dye from strong yellow to dark red. Cadmium sulfide was first synthesized in Germany in 1817 and then sold to artists as a pigment in the mid-19th century. However, its use did not become widespread until about 1917. Finely dispersed, stable, light-resistant particles have a deep color. Initial preparations of cadmium pigments had different particle sizes ranging from 0.1 to 7 micrometers, while recently obtained pigments contained only submicron particles [1]. CdS and CdO films are used as electrodes in liquid crystal displays, photodiodes, and other devices. There are few well-known wide-gap compounds and oxides that conduct currents [2-4]. Zinc oxide (ZnO), indium oxide (In_2O_3) and tin oxide (SnO_2) are the most widely known. The optical band gaps of these materials are Eg > 3 eV and they all have n-type conductivity. It is difficult to obtain ZnO films, and in order to obtain a low-resistance (In_2O_3) film, it is necessary to grow it at a temperature of about 400°C or carry out subsequent annealing [5]. This is not always

* Corresponding author: mohim@inbox.ru

© The Authors, published by EDP Sciences. This is an open access article distributed under the terms of the Creative Commons Attribution License 4.0 (https://creativecommons.org/licenses/by/4.0/).

possible. (SnO_2) films were obtained with minimal resistance at room temperature. The specific resistance of the film (SnO_2) (≈ 10^{-3} Ω · cm) is an order of magnitude higher than that of indium oxide [6]. Therefore, obtaining CdS and CdO films is an urgent task. Cadmium oxide (CdO) and cadmium sulfide (CdS) is a little studied material.

They are wide-gap semiconductors of class A^2B^6 and the transmittance of these films is quite high in the visible part. The optical band gap (Eg) of cadmium sulfide is 2.45 eV, while for cadmium oxide it varies from 2.3 to 2.7 eV [7]. We set the task to obtain and study thin films of CdS and CdO on the glass surface. When a semiconductor is illuminated, free charge carriers in the allowable bands, i.e., electrons in the conduction band and pores in the valence band, can interact with photons of energy $h\nu < E_g$. In non-polar semiconductors (Ge, Si...) at a low input concentration, free charge carriers propagate mainly by acoustic phonons. In polar semiconductors (GaAs, GaP, CdS, SiC..), at the entry points, scattering is observed both on acoustic and optical phonons. The main scattering in A^2B^6 semiconductor compounds is the propagation of optical phonons.

2 Experimental technique and results

CdO films were obtained by magnetron sputtering of a cadmium target in a mixture of argon (Ar_2) and oxygen (O_2) onto the surface of glass substrates. The pressure in the vacuum chamber was constant and amounted to $2.5\cdot 10^{-3}$ mm Hg. The partial pressure of oxygen varied from $3\cdot10^{-4}$ to $12\cdot10^{-4}$ to mm Hg. The deposition was carried out on quartz and silicon substrates at room temperature. The specific resistance of CdO films obtained on the surface of glass substrates varied from 20 Ohm·cm to 100 Ohm·cm. Resistivity was measured with the four-probe method. Different resistivity is obtained due to the partial pressure of oxygen in the vacuum chamber. The thickness of the obtained CdO films varied from 200 nm to 400 nm. And the thickness of the films depended on the sputtering time and on the power of magnetron sputtering. The essence of the method of thermal vacuum deposition can be explained as follows. The substance to be evaporated is placed in a heating device (evaporator), where it begins to evaporate intensively at a sufficiently high temperature. Under vacuum conditions created inside the chamber by special pumps, the molecules of the evaporated substance freely and quickly spread into the surrounding space, reaching, in particular, the surface of the substrate (in our case, the silicon substrate). If the substrate temperature does not exceed the critical value (Tcr), the substance condenses on the substrate, i.e., the film grows; otherwise, growth slows down or does not occur at all as a result of reverse volatilization from the surface of the substrate of the molecules or atoms of the evaporated material deposited on it. Below, we will consider the process of deposition of thin films on substrates. In fact, the speeds of atoms or molecules falling onto the substrate during deposition are quite high and, in most cases, a continuous film is obtained due to their interaction with atoms or molecules already adsorbed by the substrate. Atoms and molecules adsorbed in this way can migrate over the substrate surface, colliding with other atoms and molecules. As a result, clusters or nuclei of adsorbed atoms and molecules can appear which can be more stable than individual atoms and molecules. All these processes described above, which occur during the deposition of thin layers, can greatly affect their properties and the characteristics of the structures created on their basis. Therefore, the most important parameter of the technological process of thin film deposition is the substrate temperature, since small changes in which lead to large changes in the degree of supersaturation. With an increase in the substrate temperature, the degree of supersaturation decreases and, in this case, the average lifetime of adsorbed atoms and molecules the surface diffusion coefficient increases.

There is a certain "critical" temperature at which changes in the nucleation process are observed, above which it is difficult to obtain a high-quality film that completely and evenly covers the substrate. Therefore, to obtain high-quality films, the deposition of the latter is carried out below the critical temperature (Tcr), but close to it. At the same time, in order to avoid contamination of the deposited film with impurities located on the surface of the evaporated substance, as well as to bring the temperature of the evaporator to operating conditions, before the start of evaporation, the substrate surfaces are protected by a damper, which temporarily blocks the flow of evaporated atoms and molecules towards the substrate during heating. . The film deposition rate is directly proportional to the evaporation rate. The flux of atoms or molecules condensing on the substrate surface at fixed temperatures of the evaporator and substrate is determined by the expression [8].

$$N_p = k\frac{A}{l^2}N_i, \quad (1)$$

Where N_i is the flux of evaporating particles; l is the distance from the source to the substrate; A is the coefficient taking into account the shape and molecular-kinetic characteristics of the evaporator; k - condensation coefficient - the ratio of the number of molecules condensed on the surface of the substrate to the number of molecules that hit the surface of the substrate, numerically equal to the ratio of the rate of condensation and the rate of evaporation. Almost always, evaporation is carried out at temperatures exceeding the evaporation temperature of the substance (forced mode) in order to ensure sufficiently high vaporization rates and thereby reduce the effect of residual gases on the properties of the deposited films. At low evaporation rates, the formation of loose, rough films is possible.

The thickness of the deposited film is set by controlling the deposition time (tsp). When a predetermined value of the film thickness is reached, the flow of atoms or molecules of the substance is blocked by a damper and, at this, the film growth stops. In this case, depending on the technological process, heating of the substrate can continue or stop. During the entire technological process, a vacuum of the order of 10^{-5} Pa is constantly maintained in the chamber. To heat the evaporated substance to a temperature at which it begins to evaporate intensively, various methods are used. Basically, heating is carried out by an electron flow, laser, concentrated solar or microwave radiation, using resistive heaters, etc. In general, the vacuum deposition method is very diverse both in terms of heating the evaporated substance and in the design of evaporators. In the case when it is required to obtain films from multicomponent substances, then in this case several evaporators are used. Since the evaporation rate of different materials is different, it is rather difficult to ensure the reproducibility of the chemical composition of multicomponent films obtained by vacuum deposition. Therefore, the thermal vacuum spraying method is mainly used for single-component pure materials.

Obtaining thin films using vacuum deposition is the most interesting from the point of view of practical application, as based on them, you can create a variety of photosensitive structures with a high speed due to the small minority carrier lifetime. Studies of the crystal structure of the CdS films obtained by us by this method showed the presence of both cubic (β), and hexagonal (α) modifications. In [9] it was shown that the hexagonal phase is increased by the annealing. The transition hexagonal $\rightarrow$ cubic as a result of the elevated temperature of the substrate is observed in films up to 0.4 μm thick; at large thicknesses, mixed phases followed by an increase in the hexagonal phase and the disappearance of the cubic phase. The transformation depends on the growth rate. For its implementation, small growth rates are required.

All investigated CdS films were obtained by the method described above, i.e., by thermal spraying of powders of the binary compound CdS (semiconductor purity). CdS was

deposited slowly, as described in [10] in a quasi-closed vacuum system with a residual pressure of 10^{-5} Torr. Glass was used as substrates. However, all the same, the contaminants present on the surface of the substrates, formed as a result of long-term storage, require their removal from the surface of the substrate and its refreshment. For this purpose, we used washing, which was carried out by the displacement method [11] in two stages: first, the substrates were washed with running distilled water for 8–10 minutes, then with deionized water for 3–5 minutes. After that, the substrates were dried in an oven with infrared drying for 15–20 minutes. During film deposition, the temperature of the crucible with a source (CdS) varied in the range $T_{\mathrm{sourse}} \approx 800 \div 850$°C, and the substrate temperature was maintained within the range $T_{\mathrm{p}} \approx 250 \div 270$°C. In this case, to ensure the reproducibility of the structures, a shutter was used, with the help of which the CdS deposition time was set, which ensured that the film thickness was the same from experiment to experiment. The resulting films had a thickness w ≈ 400 nm, and an n-type conductivity with a resistivity ρ = 200 Ω cm. Next, the morphology of CdO and CdS films was studied (Figs. 1a) and 2a)). And in fig. 1 b) and 2 b) show X-ray diffraction analysis of CdO and CdS films. From the film morphology, the crystallite size was determined, which was about 50 nm for CdO films, and about 100 nm for CdS. The surface morphology of thin films was tested using an atomic force microscope (AFM) (hpAFM, Nano Magnetics). The XRD spectra of the samples were examined using an atomic force microscope and X-ray diffraction microscopy. Here we present our results as an AFM micrograph and XRD plot.

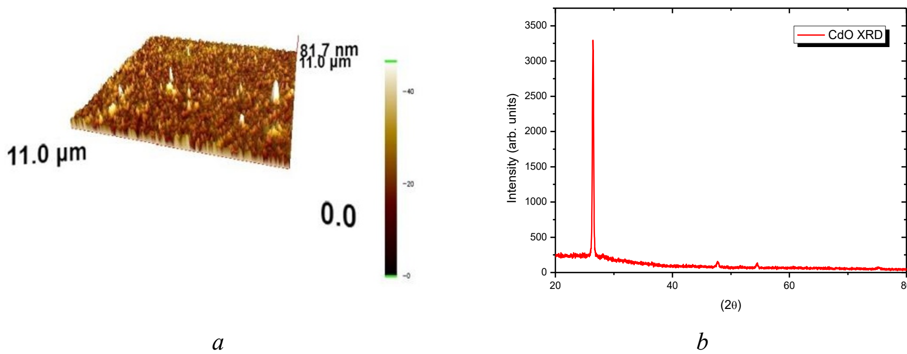

Fig. 1. (a) Micrograph of thin CdO films deposited by atomic layer deposition. (b) Wide-angle X-ray spectra of thin CdO films

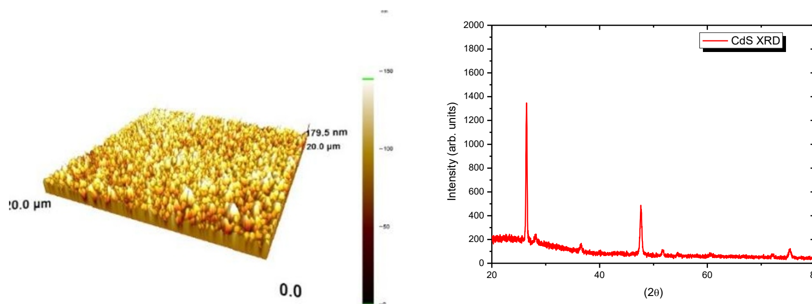

Fig. 2. (a) Micrograph of thin CdS films obtained by atomic layer coating. (b) Wide-angle emission spectra of thin CdS films

Figure 3 shows the absorption spectra of the thin films of CdO and CdS. The optical absorption of thin films was analyzed by fiber spectrometer (HR4000, Ocean Optics). These measurements allow estimating optical band gaps of the transparent thin films deposited on the surfaces of the glass substrates.

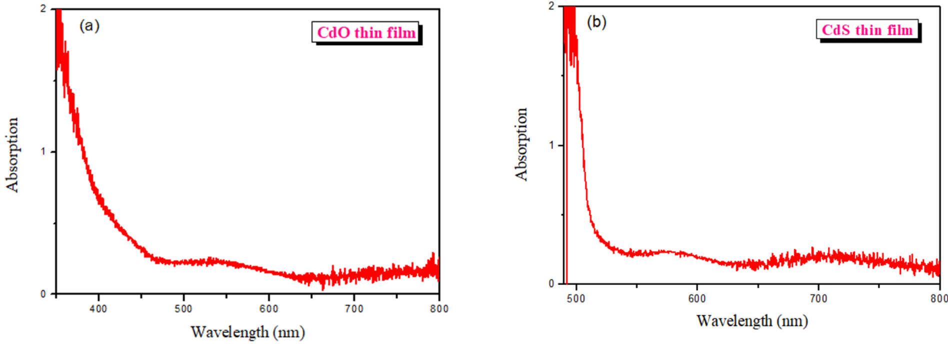

Fig. 3. Absorption spectra of thin films, which were deposited by using atomic layer deposition method: (a) CdO thin film. (b) CdS thin film

3 Analytic solutions

There are several mechanisms for absorbing light. Regardless of the mechanism of light absorption, the photon flux (light intensity) in the volume of a semiconductor decreases exponentially according to the Bouguer-Beer-Lambert law:

$$I_\nu(x) = I_{\nu 0}(1 - R_\nu)\exp(-\alpha x) \quad (2)$$

Here $I_{\nu 0}$ is the flux of n-frequency photons incident on the semiconductor surface, $I_{\nu 0}(1 - R_\nu)$ is the flux of photons incident on the semiconductor, R_ν is the reflection coefficient, and a is the absorption coefficient. Depending on what the energy of absorbed photons is directly used for, the mechanisms of optical absorption can be divided into specific, exciting, introductory, lattice (phonon), plasma, and free charge carriers.

$$\alpha(h\nu) = -\frac{\left(\frac{dI_\nu(x)}{dx}\right)}{I_\nu(x)} \quad (3)$$

The image of formula (3) is the energy absorbed per unit of time by a unit of volume. Therefore, for any optical transitions, we write formula (3) in the form (4).

$$\alpha(h\nu) = -\frac{N(h\nu) * h\nu}{I_{\nu 0}} \quad (4)$$

The absolute number (probability) of interzonal electronic transitions occurring in the same volume per unit time under the action of the light wave field in expression (4) $N(h\nu)$:

$$N(h\nu) = \frac{2}{(2\pi)^3}\int d^3k_j \int W_{jf} * [f(k_j) - f(k_f)]d^3k_j \quad (5)$$

$k_f, k_j -$ are wave vectors, $f(k_f), f(k_j)$ respectively (3.4) are functions representing the initial and final states of the integral. $\alpha(h\nu)$ spectral connection between bands $E_V \rightarrow E_C$essentially depends on the nature of the transitions.

 https://doi.org/10.1051/e3sconf/202341002057

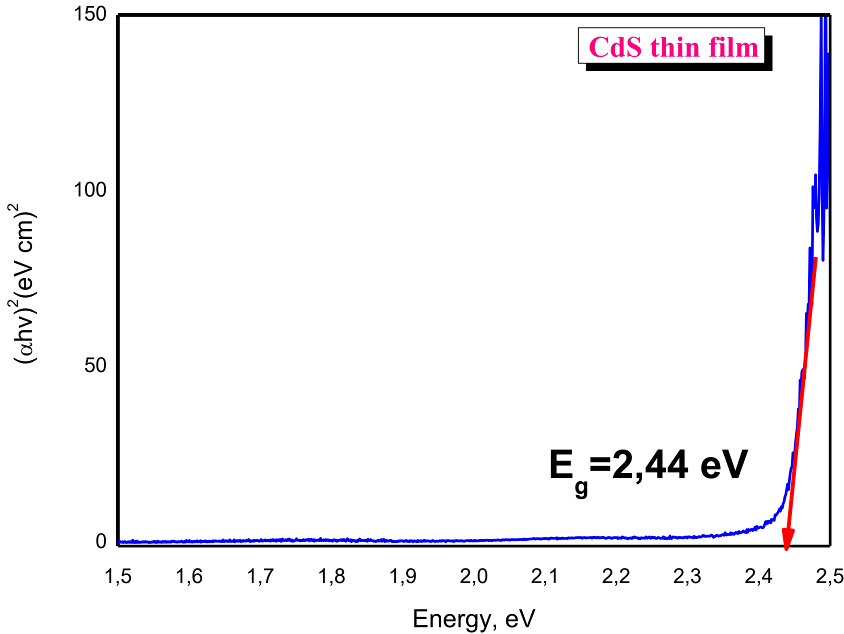

Fig. 4. Shows the dependence of the absorption coefficient of the CdS material on the photon energy according to the The Tauc's model

To determine the expression $\alpha(h\nu)$the energy of optical transitions is written as follows.

$$h\nu = E_g \pm \frac{h^2k^2}{2m^*} \tag{6}$$

where m^* is the effective mass, E_g –is the bandwidth of the forbidden field (5) and (6) can be solved together by substituting (4) into expression (7) We obtain the following expressions (7) for allowed and forbidden transitions.

$$\alpha(h\nu) = \frac{A_1(h\nu - E_g)^{\frac{1}{2}}}{h\nu} \quad \text{and} \quad \alpha(h\nu) = \frac{A_1(h\nu - E_g)^{\frac{3}{2}}}{h\nu} \tag{7}$$

$A_{1,}A_2$ –Coefficients that do not depend on the of frequency but include the parameters of the zones involved in optical transitions and some international constants.

4 Conclusions

In the transitions that occur with the release or absorption of a photon, we can see that the electron passes from the initial valence band $E_j, and\ k_j$ to the transient state $E_f, and\ k_f$under the action of the photon, which can be considered as a two-step process. We can see that the coefficients $A_{1,}A_2$also depend on the concentration of ionized acceptors in some semiconductors. From the film morphology, the crystallite size was determined, which was about 50 nm for CdO films, and about 100 nm for CdS. The surface morphology of thin films was tested using an atomic force microscope (AFM) (hpAFM,

Nano Magnetics). The XRD spectra of the samples were examined using an atomic force microscope and X-ray diffraction microscopy.

References

1. Thoury, M., Delaney, J. K., de la Rie, E. R., Palmer, M., Morales, K., & Krueger, J. Near-infrared luminescence of cadmium pigments: in situ identification and mapping in paintings. Applied Spectroscopy, Vol. 65(8), pp.939-951 (2011).
2. Hartnagel, H. L., Dawar, A. L., Jain, A. K., & Jagadish, C. Semiconducting Transparent Thin Films. MRS BULLETIN. (1997).
3. Mirsagatov, S. A., & Sapaev, I. B. Mechanism of charge transfer in injection photodetectors based on the M (In)-n-CdS-p-Si-M (In) structure. Physics of the Solid State, 57, 659-674. (2015).
4. Mirsagatov, S. A., Sapaev, I. B., Valieva, S. R., & Babajanov, D. Electrophysical and Photoelectric Properties of Injection Photodiode Based on pSi–nCdS–In Structure and Influence of Ultrasonic Irradiation on them. Journal of Nanoelectronics and Optoelectronics, Vol. 9(6), pp.834-843. (2015).
5. Bales, G. S., Bruinsma, R., Eklund, E. A., Karunasiri, R. P. U., Rudnick, J., & Zangwill, A. Growth and erosion of thin solid films. Science, 249(4966), pp.264-268. (1990).
6. Webb, J. B., Williams, D. F., & Buchanan, M. Transparent and highly conductive films of ZnO prepared by rf reactive magnetron sputtering. Applied Physics Letters, 39(8), 640-642. (1981).
7. Chu, T. L., & Chu, S. S. Degenerate cadmium oxide films for electronic devices. Journal of electronic materials, 19, 1003-1005 (1990).
8. Sravani, C., Reddy, K. R., & Reddy, P. J. Preparation and properties of CdO/CdTe thin film solar cells. Journal of Alloys and compounds, Vol. 215(1-2), pp.239-243. (1994).
9. Kobeleva, S. P., Anfimov, I. M., Berdnikov, V. S., & Kritskaya, T. V. Possible causes of electrical resistivity distribution inhomogeneity in Czochralski grown single crystal silicon. Modern Electronic Materials, Vol. 5(1), pp. 27-32. (2019).
10. Brewer, G. (Ed.). Electron-beam technology in microelectronic fabrication. Elsevier. (2012).
11. Ohring, M. Materials Science of Thin Films: Depositon and Structure. Elsevier. (2001).